Supplementary information for

Strong two-photon and three-photon absorptions in the antiparallel dimer of a porphyrin–phthalocyanine tandem

Mitsuhiko Morisue,[‡,§] Kazuya Ogawa,*[‡,∞] Kenji Kamada,*[≠] Koji Ohta,[‡≠] and Yoshiaki Kobuke*[‡,#]

[‡]*Graduate School of Materials Science, Nara Institute of Science and Technology, 8916-5 Takayama, Ikoma, Nara 630-0192, Japan.*
[≠]*Photonic Research Institute, National Institute of Advanced Industrial Science and Technology (AIST), 1-8-31 Midorigaoka, Ikeda, Osaka 563-8577, Japan.* E-mail: k.kamada@aist.go.jp
[§]Present address: Department of Biomolecular Engineering, Kyoto Institute of Technology, Matsugasaki, Sakyo-ku, Kyoto 606-8585, Japan.
[∞]Present address: *Interdisciplinary Graduate School of Medical and Engineering Division of Medicine and Engineering Science, Life Environment Medical Engineering, University of Yamanashi, 4-3-11 Takeda, Kofu, Yamanashi 400-8511, Japan.* E-mail: kogawa@yamanashi.ac.jp
[#]*Present address: Institute of Advanced Energy, Kyoto University, Gokasho, Uji, Kyoto 611-0011, Japan. E-mail: kobuke@iae.kyoto-u.ac.jp*

Measurements of two-photon absorption (2PA) spectra

The open-aperture Z-scan method was used for nonlinear absorption measurements. An optical parametric amplifiler (Spectra-Physics OPA-800) pumped by a femtosecond regenerative amplifier system (Spectra-Physics Spitfire, 120–135 fs, 1 kHz) was used as a light source. The details of our measurement setup were reported previously.[S1] At one wavelength, several scans were recorded for each sample by varying the average incident power below 0.4 mW. This incident powers approximately correspond to the on-axis peak intensity I_0 of 150 GW/cm^2 or less. The procedure was repeated for different wavelengths in order to obtain a spectrum.

Data analysis of the open-aperture Z-scan traces

The obtained open-aperture Z-scan traces were analyzed by our standard procedure.[S1,S2] The procedure is explained here briefly. To each trace, the curve fit based on the following equations was applied:

$$T_N(\zeta) = \frac{(1-R)^2 \exp(-\alpha L)}{\sqrt{\pi}\, q(\zeta)} \int_{-\infty}^{+\infty} \ln\left[1+q(\zeta)\exp(-x^2)\right] dx \quad (1)$$

with

$q(\zeta) = q_0/(1+\zeta)^2$

and the normalized sample position

$\zeta = (z - z_0)/z_R$

Eq. 1 stands for the energy transmittance of a spatially and temporally Gaussian pulse through a 2PA active media. Here, T_N is the energy transmittance normalized to its value at an off-focus (practically, at an end of the scan, where $z - z_0 >> z_R$). From the curve fit, the set of parameters (q_0, z_0, z_R) was obtained for the scans with different incident powers. However, the values of the focal position z_0 and the Rayleigh range z_R are defined by the optical configuration, and are independent of the incident power. Thus, the global fitting with z_0 and z_R as global parameters was performed for the set of traces with different incident powers. This global fitting procedure improves reliability of analysis when the signal-to-noise ratio is poor. The 2PA absorbance q_0 is defined as

$$q_0 = \beta(1-R)I_0 L_{\text{eff}} \quad (2)$$

where β is the 2PA coefficient. So, q_0 is proportional to I_0. β was calculated from the plot of q_0 against the incident power, *i.e.*, against to I_0. (Here, R is Fresnel reflectance at the cell surface, L_{eff} is the effective path length defined as $L_{\text{eff}} = \{1-\exp(-\alpha L)\}/\alpha$, α is the linear absorption coefficient and L is the physical path length of the cell. L_{eff} is reduced to L when linear absorption is negligible.) The 2PA cross section was calculated by $\sigma^{(2)} = \hbar\omega\beta/N$ with the number density N.

Data analysis by considering saturable absorption

Saturable absorption, suppression of linear absorption by reduced difference in population between the ground and excited states under intense laser irradiation, could be, but not always, observed when the linear absorption of the sample was not negligible. It was observed as increase in transmittance with increasing the incident optical intensity. In open-aperture Z-scan traces, it was recorded by a bump centered at the focal point ($z = z_0$), or more complicatedly, two bumps beside the depression at the focal point when 2PA was observed in addition to the saturable absorption.

Saturable absorption can be treated phenomenologically by introducing intensity-dependent linear absorption coefficient:[S3]

$$\alpha(I) = \frac{\alpha}{1 + I/I_S} \quad (3)$$

where is I the incident intensity and I_S is the saturation intensity. It is clear from Eq. 3 that $\alpha(I)$ drops to its half value $\alpha(I_S) = \alpha/2$ when $I = I_S$. In order to apply Eq. 3 to the analysis of the Z-scan traces, it is be rewritten as a function of the normalized sample position ζ as,

$$\alpha(\zeta) = \frac{\alpha}{1 + \left(\frac{I_0}{I_S}\right)\left(\frac{1}{1+\zeta^2}\right)} \quad (4)$$

Here, it should be recalled that we assume the Gaussian beam. Now, α in Eq. 1 was replaced with Eq, 4. The Global fitting procedure using this modified equation was applied for the recorded traces with different incident powers (*i.e.*, different I_0). z_0, z_R, α and I_S were treated as global fitting parameters. The recorded Z-scan traces of both compounds, *i.e.*, H_2(ImPor)-Zn(Pc) and Zn(ImPor)-Zn(Pc), at 844 and 872 nm

exhibited sign of saturable absorption (Figure S1), so they are analyzed this global fitting procedure. The obtained 2PA cross sections with this analysis smoothly connect to those at the longer wavelength where no saturable absorption is observed (Figure 5 in the main text).

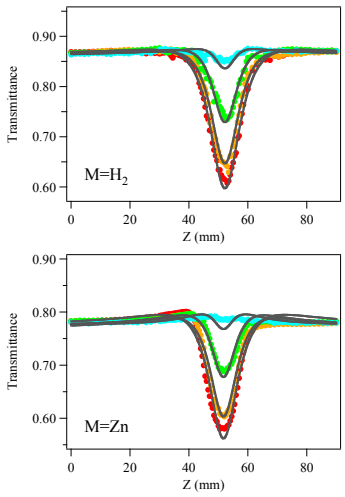

Figure S1. The open-aperture Z-scan traces of M(ImPor)-Zn(Pc) at 844 nm with different incident powers (circles) and curve fits based on Eq. 1 with Eq. 4 (gray curves).

For fully consistent treatments, α must be replaced with $\alpha(I)$ for the calculation of β using Eq. 2 because L_{eff} contains α. However, this is technically difficult for the current analysis scheme. Thus α leaves as a constant value for the calculation of β using Eq. 2. This overestimates the β value at most by 10%. However this error does not seem to be important because that is comparable or smaller than the measurement error.

Data analysis for three-photon absorption (3PA)

As shown in Figure 4a in the main text, the quadratic relationships between q_0 and I_0 suggest the existence of higher-order nonlinear absorption. Thus, the open-aperture traces were re-analyzed based on a 3PA model. In this case, the normalized transmittance for 3PA process is described by the following equations:[S4]

$$T(\zeta) = \frac{(1-R)^2 e^{(-\alpha^{(1)}L)}}{\sqrt{\pi}\,p(\zeta)} \int_{-\infty}^{\infty} \ln\left[\sqrt{1+p(\zeta)^2 e^{(-2x^2)}} + p(\zeta)e^{(-x^2)}\right]dx \quad (5)$$

$$p(\zeta) = \frac{p_0}{1+\zeta^2} \quad (6)$$

where the 3PA parameter p_0 is defined as

$$p_0 = (2\alpha^{(3)}L'_{\mathrm{eff}})^{1/2}(1-R)I_0 \quad (7)$$

where $\alpha^{(3)}$ is the 3PA coefficient, L'_{eff} denotes the quadratic effective path length defined as $L'_{\mathrm{eff}} = \{1 - \exp(-2\alpha^{(1)}L)\}/2\alpha^{(1)}$. The parameter p_0 was obtained by curve fitting to the observed traces with Eqs. 5 and 6. For 3PA, another linear relationship is expected between p_0 and I_0 as in Eq. 7. The obtained p_0 was found to exhibit good linear relationship against I_0 (Figure 4b, in the main text). The $2\alpha^{(3)}$ was obtained from a plot of p_0 versus I_0 based on Eq. 7, and then the 3PA cross section $\sigma^{(3)}$ was given by

$$\sigma^{(3)} = (\hbar\omega)^2\alpha^{(3)} \quad (8)$$

The above discussion is rigorous when 3PA process is exclusively involved in the observation. As mention in the main text, it is not easy to distinguish 2PA and 3PA when both process are involved in the observation because both process are intensity-dependent. One of the simplest and practical way to estimate the contribution of 2PA in such case is to treat the data at low incident power where the 3PA process is ignored. Therefore, we took the data at < 0.2 mW for the estimation of 2PA cross section at the wavelengths in which 3PA was observed.

Structural characterization of Zn(ImPor)-Zn(Pc)

We previously reported the synthesis and structural characterization of H_2(ImPor)-Zn(Pc).[S5] A solution of H_2(ImPor)-Zn(Pc) in chloroform (5 mL) was treated with saturated zinc acetate in methanol (2 mL) for zinc insertion. After stirrig for 10 h at room temperature, the solution was successively washed with aqueous saturated sodium hydrogencarbonate and brine. The organic layer separated was dried over anhydrous sodium sulfate. Zn(ImPor)-Zn(Pc) was eluted from a silica-gel column chromatography with chloroform/methanol (9/1, v/v). Zn(ImPor)-Zn(Pc) was obtained quantitatively as green substance. ^{1}H NMR of Zn(ImPor)-Zn(Pc) showed no substantial change from that of H_2(ImPor)-Zn(Pc),[S5] other than the disappearance of innner protons of the Por ring around -2.5 ppm. Complete assignment

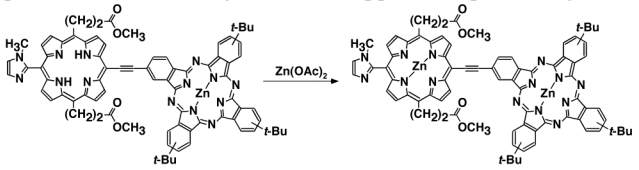

Scheme S1. Synthesis of Zn(ImPor)-Zn(Pc) derived from zinc H_2(ImPor)-Zn(Pc).

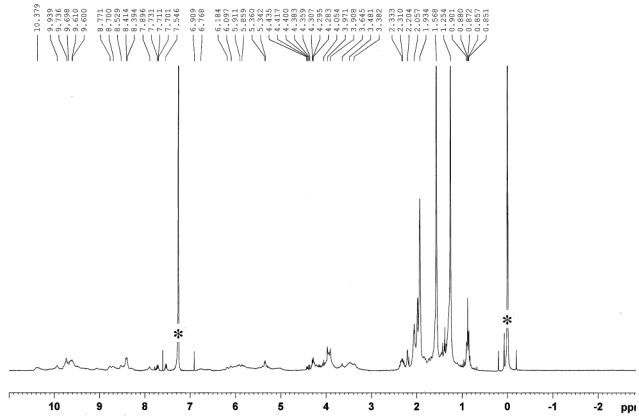

Fig S2. ^{1}H NMR spectrum (300 MHz) of Zn(ImPor)-Zn(Pc) in $CDCl_3$. Asterisk indicates the signals of residual solvent and TMS as an internal standard.

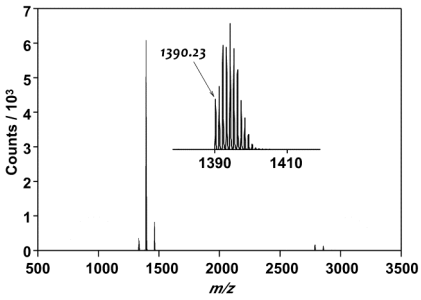

Fig S3. MALDI-TOF MS spectrum of Zn(ImPor)-Zn(Pc) in dihranol as a matrix.

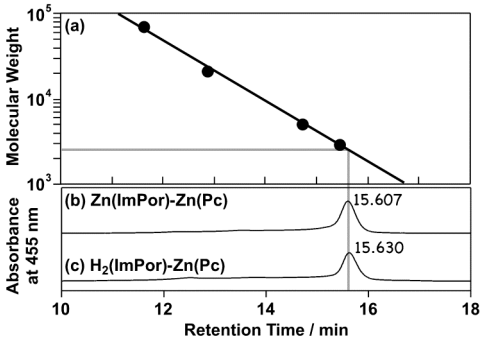

Fig S4. (a) Logalithmic plot of molecular weight with reference to polystyrene as a standard (open circle). Size-exclusion chromatographic traces of (b) Zn(ImPor)-Zn(Pc) and (c) H_2(ImPor)-Zn(Pc) with chloroform as the eluent. SEC was monitored at 455 nm with an eluting flux of 1 mL/mim by a LC-NetII/ADC (JASCO) equipped with Shodex KF-802.5 and KF-804L (Showa Denko).

of protons were difficult due to the existence of the isomers with several substitution patterns of *tert*-butyl groups and stacking configuration (Fig S2), as described in our previous report.[S5] ^{1}H NMR (300 MHz) in $CDCl_3$: δ = 1.93-2.06 (m, 27H; *tert*-Bu), 2.31, 2.33 (s, s, 3H; imidazolyl-*N*CH_3), 3.38-3.64 (m, 4H; 4-imidazolyl and -COOCH_3), 3.91-4.43 (br m, 4H; Por-CH_2CH_2COOMe), 5.34-6.18 (br m, Por-CH_2CH_2COOMe and α-positions of Pc ring), 7.54-10.38 ppm (br m; α-positions of Pc ring and β-positions of Por ring). MALDI-TOF MS: m/z: calcd: 1390.40; found: 1390.23 (Fig S3).

Analytical size-exclusion chromatograms of Zn(ImPor)-Zn(Pc) showed the peak at the retention time identical with that of H_2(ImPor)-Zn(Pc) (Fig S4), corresponding the molecular weight of the dimer of a tandem. Close similarity of the retention time suggests that both tandem adopts the same configuration of the dimer.

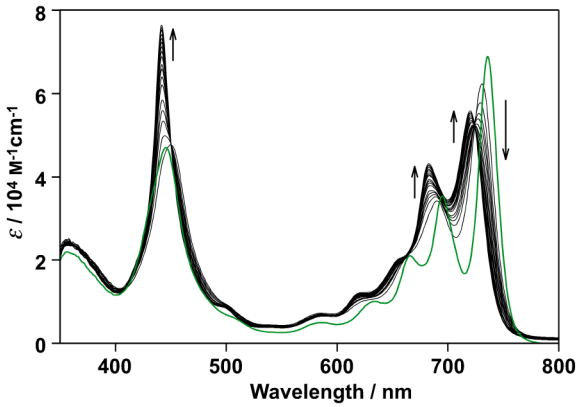

Fig S5. Spectral titration of Zn(ImPor)-Zn(Pc) with 1-methylimidazole in toluene at 25 °C (recorded on addition of every 1400 equivalent of 1-methylimidazole). Green line indicates the initial spectra.

On the titration experiment with 1-methylimidazole, Zn(ImPor)-Zn(Pc) showed spectral change, even through no isosbestic points (Fig S5). Susceptibility of Zn(ImPor)-Zn(Pc) to 1-methylimidazole as the competitive ligand indicates that Zn(ImPor)-Zn(Pc) formed the organized structure through imidazolyl-to-zinc coordination. Furthermore, no appreciable splittings of porphyrin Soret band excludes the possible existence of homo-cofacial stack of the Zn(ImPor)-Zn(Pc) in the absence of 1-methylimidazole.[S6] Combining the whole results of ^{1}H NMR, SCE, and the spectral shape in the absorption, it is assumed that the organized structure of Zn(ImPor)-Zn(Pc) is dominantly converged to the hetero-stacked structure through complementary coordination. This assumption is compatible with the fact that imidazolyl-to-Zn(Pc) self-complementary coordination is 1000 times stronger than imidazolyl-to-Zn(Por).[S5,S7]

Notes and references

[S1] K. Kamada, K. Matsunaga, A. Yoshino, K. Ohta, *J. Opt. Soc. Am. B*, 2003, **20**, 529–537.
[S2] K. Kamada, K. Ohta, Y. Iwase, K. Kondo, *Chem. Phys. Lett.* 2003, **372**, 386–393.
[S3] R. L. Sutherland, in "*Handbook of Nonlinear Optics*", 2nd Ed., Mercel Dekker, Inc. New York, 2003, p.463.
[S4] R. R. Tykwinski, K. Kamada, D. Bykowski, F. A. Hegmann, R. J. Hinkle, *J. Opt. A: Pure Appl. Opt.* 2002, **4**, S202, and references therein.
[S5] M. Morisue, Y. Kobuke, *Chem. Eur. J.* 2008, **14**, 4993–5000.
[S6] A. Satake, T. Sugimura, Y. Kobuke, *J. Porphyrins Phthalocyanines* 2009, **13**, 326–335.
[S7] K. Kameyama, M. Morisue, A. Satake, Y. Kobuke, *Angew. Chem. Int. Ed.* **2005**, *44*, 4763–4766.